

**Implementation of Constitutive Equations for Viscoplasticity  
with Damage and Thermal Softening into the LS-DYNA Finite  
Element Code, with Application to Dynamic Fracture of Ring-  
Stiffened Welded Structures**

**Ricardo F. Moraes - Ph. D. Candidate**

Major of the Army of Brazil

Sponsored by the Brazilian Government CNPq – IME

Mechanical, Material and Aerospace Engineering,

University of Central Florida, Orlando,

P. O. Box 162450, FL 32816-2450

E-mail: rfm93635@pegasus.cc.ucf.edu

**David W. Nicholson – Ph. D. - Professor**

Mechanical, Material and Aerospace Engineering,

University of Central Florida, Orlando,

P. O. Box 162450, FL 32816-2450

E-mail: nicholsn@pegasus.cc.ucf.edu

*Abbreviations:*

CDM	Continuum Damage Mechanics
D	Damage Parameter
FE	Finite Element
HAZ	Heat Affected Zone
RVE	Reference Volume Element
UMAT	User Defined Material

*Keywords:*

Damage, User Defined Material, Viscoplasticity, Welds

## ABSTRACT

Constitutive equations for a viscoplastic model with damage and thermal softening are implemented in the Finite Element (FE) code LS-DYNA using a *User Defined Subroutine* UMAT. A modified Johnson-Cook constitutive model, UMAT 15, which accounts for strain rate viscoplastic effects, is used. The Continuum Damage Mechanics (CDM) is based on Bonora formulation (Bonora, 1997). The combined material model, named UMAT 41, is added to the program static library using Digital Visual Fortran (FORTRAN 90). A brief procedure on how to implement a UMAT is also briefly discussed in this work.

Using the User Defined Material, the solution of an explosive charge applied to a ring-stiffened welded structure is analyzed. This type of structure is widely used in ships and aircraft, which are subject to explosive or projectile attack. Results obtained using models with and without damage softening agree very well with previously published data with respect to crack paths. However, the time histories and thresholds are sensitive to the model used.

## INTRODUCTION

The majority of large modern metallic structures such as ships use welding as an essential process during assembly. Unfortunately, metallurgical control is very limited in welded regions and, because of the welding process, the mechanical properties differ significantly all through the region. The heat input produces a *Heat Affected Zone* (HAZ) with significant variation in hardness (Giovanola et. al., 1993). Welds frequently incorporate defects such as voids due to *lack of penetration*. So, it becomes clear that the weldment may contain structural weak points. Accordingly, it is important to evaluate their fracture resistance under realistic loading conditions. Of particular interest here are impulsive loads, generated by explosive charges, projectile impact or other high strain rates phenomena encountered in ballistic or crash scenarios. This class of loadings gives rise to what is known as dynamic fracture.

The two goals of the numerical investigation are (a) to accommodate *Damage Softening* in structures that experience ductile fracture due to an impulsive loading such as projectile impact or an explosive charge (Giovanola et. al., 1991) and (b) to simulate dynamic fracture of weldments in stiffened structures. A constitutive model (Johnson et. al., 1983), which is sensitive to strain rate effects and temperature softening, is extended to explain the proposed idea. A model that introduces a damage-modified value for the equivalent stress and for the yield stress is also proposed. The equations are derived through continuum mechanics concepts. Continuum Damage Mechanics (CDM) was first introduced during the fifties. Since then, the topic has been under development by many authors. Phenomenologically, damage represents an intermediate condition between an ideal material and macroscopic crack initiation (Kachanov, 1986). Numerical simulations are performed in the explicit finite element impact code LS-DYNA (Hallquist, 1993). An extension of the Johnson-Cook thermoviscoplastic model to include damage has been implemented through the User Defined Material Interface.

After the current investigation had started, version 9.5 of LS-DYNA was released with a new model incorporating damage. However, it does not also accommodate temperature effects nor has been applied to weldments (Berstad et al., 1999).

## STATEMENT OF THE PROBLEM

The weldment structure assumed is based on symmetric and asymmetric weld fillets. The assembly consists of a base plate and two stiffeners (Giovanola et. al., 1993). A vertical impulsive load simulation is applied as represented in Figure 1. This load is generated by an explosive charge.  $V_0$  is the initial velocity of the base plate and is a function of the type and quantity of the explosive used. This structure is important to ring-stiffened cylindrical pressure vessels, submarine structures and others. In the present work, simulations are performed on both symmetric and asymmetric welds. Results are compared with previous data.

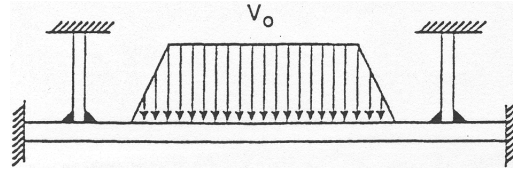


Figure 1: Assembly for numerical simulation of symmetric weldment

Figure 2 represents the weld geometry for the symmetric and asymmetric fillets (Figures *a* and *b*, respectively). Figure 2 also represents the different material regions generated during the weld process. In order to perform simulations, it is necessary to estimate strength and fracture properties in the weldment region. The values used in this work are based on the data presented by previous authors (Giovanola et. al., 1993, Giovanola et. al., 1991) and are assumed to be reliable. Table 1 shows the properties for the different materials/regions of Figure 2. Simulation is also performed for the material 4340, for which properties are listed in Table 2. They are quoted from the code EPIC II.

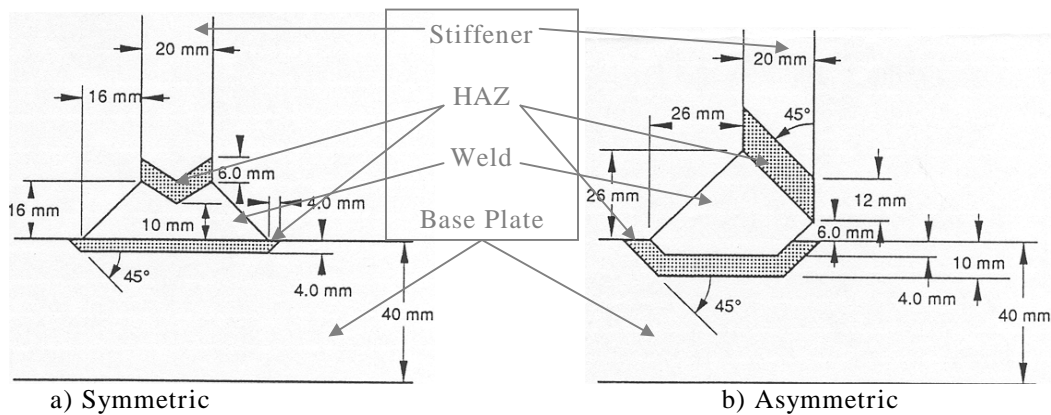


Figure 2 – Weld geometry

Table 1: Material Properties - Giovanola et al. (1991)

Zone	High strength Yield Stress (MPa)	Low strength Yield Stress (MPa)
Base	930	800
Stiffener	930	620
Weld	744	800
HAZ	1116	930

Table 2: Properties for simulation - Material 4340

Zone	A MPa	B MPa	C	n	m
Base Plate	792	510	.014	.26	1.03
Stiffener	792	510	.014	.26	1.03
Weld	634	408	.014	.26	1.03
HAZ	954	615	.014	.26	1.03

## PROCEDURE TO DEVELOP UMAT

The development of an User Defined Material in LS-DYNA is easy. The next several paragraphs detail how this task can be accomplished in a PC based version.

A static library version of LS-DYNA is needed as well as the make-up file necessary to create a workspace. The company KBS2 gave access to the necessary files for the current study in Feb/99. LS-DYNA is written in FORTRAN with some subroutines written in C. The user needs to create new subroutines. Once the new subroutines are finished, the user has to link them with the static library through the make-up file to create a new LS-DYNA executable file.

The user has to know a priori the necessary capabilities of his/her UMAT. Furthermore, the user has to know exactly which variables (temperature, accumulated plastic strain, etc.) have to be transferable from the main program to the UMAT, and make sure that the files provided are able to handle it. If the requested static library does not accommodate a required variable, temperature for instance, then a new static library must be obtained.

The UMAT is called at each material integration point at every time step of each increment. When it is called, the UMAT is provided with the material state, i.e., stress, strain, strain rate and other tensors. A central difference method is used to do the time integration at each time step in order to update the quantifiers of interest. The damage and the failure parameter are treated as history variables stored in a specific file. LS-DYNA allows a maximum of ten (10) simultaneous User Defined Material Subroutine (UMAT) and forty-eight (48) history variables for each UMAT. The communication between the static library of the main program, the User Defined Material UMAT, the additional user's subroutines, the pre-processor and the post-processor is represented in Figure 3.

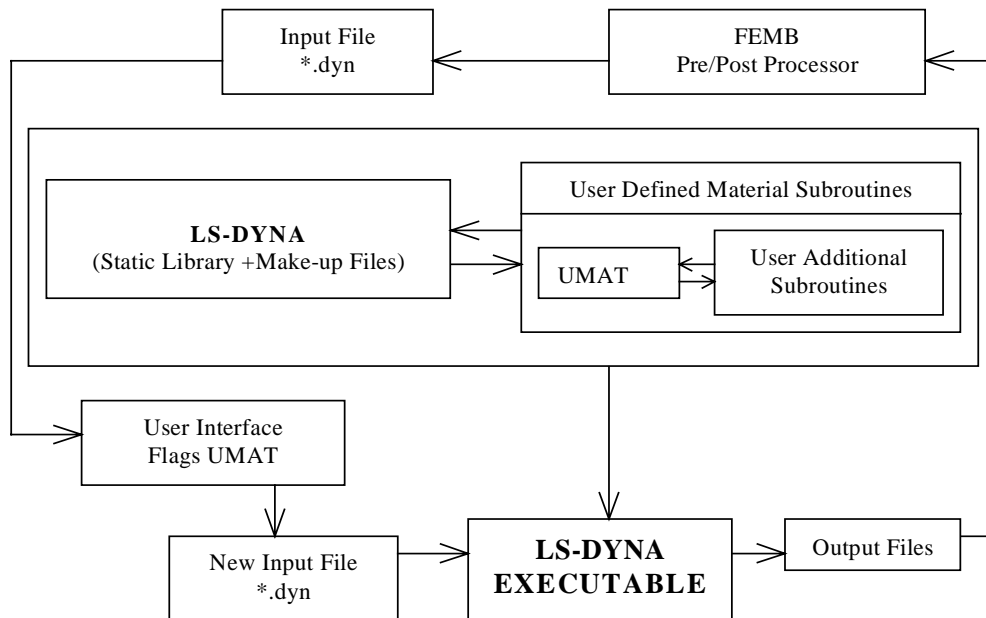


Figure 3 – Communication between LS-DYNA and separate files

## CONTINUUM DAMAGE MECHANICS

### *Basic Concepts*

Damage mechanics represents the microstructural deformation and the failure process in terms of continuum parameters averaged over a small volume of material. Therefore, the model focuses on processes in the damaged zone itself. Damage can be simply viewed as the intermediate process between a virgin material and macroscopic crack initiation.

Before discussing damage softening, it is important to understand that the material under analysis can be studied at three different levels:

- Microscale: Analysis of the accumulation of microstresses in the neighborhood of defects or interfaces and the breaking of bonds. Study of strain and damage.
- Mesoscale: Analysis of the growth and coalescence of microvoids that will give origin to a crack. Establishment of constitutive equations.
- Macroscale: Analysis of the growth of the crack initiated at the mesoscale level. Crack propagation.

The first two levels may be studied by damage variables of CDM (Lemaitre, 1996). The third stage is usually studied using fracture mechanics. It is at the mesoscale level that the Reference Volume Element (RVE) is established. Damage can be coupled to elastic and to plastic response.

Bonds between atoms hold materials together. When debonding occurs, the damage process starts. This damage process directly influences elasticity, since the number of atomic bonds is responsible for the elastic parameters established at a mesoscale level. In particular, the elastic moduli decrease with the increase of damage. Normally the constitutive equations of a material are written at a mesoscale level, incorporating properties of linearity and isotropy, which reflect atomic bonds discussed above.

Because plasticity corresponds to crystal slip, *there is no fundamental coupling between plasticity and damage*. In metals, slips occur primarily by movements of dislocations. Dislocation may move by the displacement of bonds, thus creating a plastic strain by slip only, i.e., without any debonding. *Any apparent coupling between damage and plasticity is due to a damage-induced increase of the effective stress*.

At low levels of stresses in elasticviscoplastic materials, the Cauchy stress tensor  $\sigma_{ij}$  is dependent only of the state of strain. Depending on the strain rate and above certain levels of stress, denominated as the yield stress  $\sigma_y$ , permanent plastic deformations are obtained. The value of the yield stress changes with increasing plastic deformation and with the rate of this same deformation. Assume for example a 1-D tensile test, where the phenomena of elasticity, plasticity and viscoplasticity are represented in Figure 4.

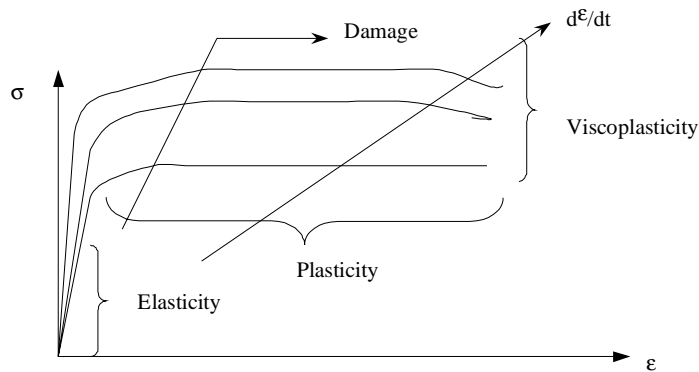


Figure 4 – representation of elasticity, plasticity and viscoplasticity

The type of damage of interest here is known as *Ductile Plastic Damage*. This type has particular interest for the dynamic applications under consideration in this work. It involves the nucleation of cavities due to debonding, followed by their growth and coalescence ensuing from plastic instability in the 'ligaments' between damaged zones. Figure 5 depicts damage, and its effect on plastic instability (negative stiffness).

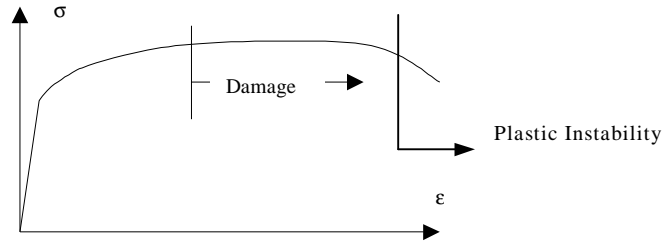


Figure 5: Representation of ductile damage

A variable damage parameter,  $D$ , is introduced to explain this property and it satisfies:

- $D=0$ , represents an undamaged state
- $D=1$ , implies rupture of the element
- $0 < D < 1$ , measures the current damaged state

Regarding  $D$ , the model developed by Bonora (Bonora, 1997), for instance, is based on the work published by Lemaitre (Lemaitre, 1985) and assumes the following:

- Isotropic Damage
- Effective Stress
- Equivalent Strain
- Thermodynamical Damage Potential

*Isotropic Damage Hypothesis* states that the variable  $D$  can be fully represented by a scalar. As a hypothesis, damage is assumed measurable as a quantity, which is a unique continuous value over the RVE. Doing so, it is assumed that the deterioration in the zone where damage occurs can be 'smeared' in all directions. Therefore, in this case, the value of  $D$  is to be understood in the sense of averaging. Figure 6 illustrates this notion. Hence, damage is treated as an isotropic value, i.e., a scalar variable. In the general anisotropic case, this damage variable should be represented by a fourth order tensor  $D_{ijkl}$ . In the current work, the isotropic scalar hypothesis will also be assumed.

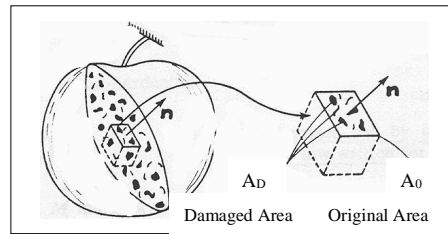


Figure 6: Concept of isotropic damage

At this point, the variable damage,  $D$ , can be fully defined as,

$$D = \frac{A_D}{A_0} ; \quad 0 \leq D \leq 1 \quad (1)$$

*Effective Stress Hypothesis* states that the following equation relates the true stress acting on the damaged material element to the stress of the undamaged material element:

$$\tilde{\sigma} = \frac{\sigma}{1 - D} \quad (2)$$

*Equivalent Strain Hypothesis* states that the strain behavior is modified by damage which is dependent only on the effective stress.

*Thermodynamic Potential Hypothesis* assumes the existence of a potential function of observable and internal variables. Following Bonora, this potential is decomposed as

$$\psi = \psi_e(\boldsymbol{\varepsilon}^e, T, D) + \psi_p(T, p) \quad (3)$$

where the internal variables are the accumulated plastic strain  $p$  and the damage  $D$ . The observable variables are the elastic strain tensor  $\boldsymbol{\varepsilon}$  and the temperature  $T$ . Note that damage and plastic strain are uncoupled at a microscopic scale.

During the last three decades, many authors have presented theories intended to explain ductile fracture using a local criterion approach (Mudry, 1985). The model of Equation 4 shows an integral equation that evaluates the damage, as a function of plastic strain, over a small volume of material.

$$D = \int \frac{d\varepsilon_{eq}^p}{\varepsilon_c \left( \frac{\sigma_m}{\sigma_{eq}} \right)} \quad (4)$$

Here  $D$  is a damage function assumed to depend on the ratio of the incremental von Mises equivalent plastic strain and a critical experimental strain, given by a function of the ratio of the mean stress to the von Mises stress. This latter ratio is also known as the stress triaxiality factor. Failure occurs when  $D$  equals unity. At the boundaries of inclusions, non-homogeneous zones, or at crack tips, high values of stress triaxiality and steep strain gradients are expected.

#### *Damage Softening*

In the past many authors endeavored to explain the material behavior at high strain rates using the concept of thermal softening. Bamman (Bamman, 1990) presented a strain rate and temperature dependent plasticity model for finite deformation. Here, for the sake of comparison, thermal softening concepts are discussed and illustrated using experimental data from the literature.

Johnson-Cook (Johnson-Cook, 1983) introduces in the third term of Equation 5 a capability for accommodating thermal softening, based on a large body of experimental data. In his work, the coupling between the thermal softening fraction term  $K_T$  and the strain rate term is discussed. In this work, we introduce the idea of damage softening analogous to thermal softening, making use of the effective stress concept.

## MATERIAL MODELS

#### *Johnson-Cook*

Equation 5 shows the Johnson-Cook relation, giving the flow stress in terms of plastic strain, strain rate and temperature. The plasticity in this model is sensitive to strain rate and temperature. This type of material is particularly suitable if strain rates vary over a large range, and if there are significant adiabatic temperature increases due to plastic heating. Note the thermal softening capability.

$$\sigma = \left[ A + B\varepsilon^n \right] \left[ 1 + C \ln \dot{\varepsilon}^* \right] \left[ 1 - T^{*m} \right]. \quad (5)$$

Note: the damage parameter,  $D$ , does not appear in Equation 5. The strain at fracture is calculated separately using

$$\epsilon^f = [D_1 + D_2 \exp D_3 \sigma] [1 + D_4 \ln \epsilon^*] [1 + D_5 T^*] \quad (6)$$

where  $D_1 \dots D_5$  are material constants. It is important to recall that in the Johnson-Cook model do not consider damage. In this particular model damage, softening is not accommodated and failure is predicted using a separate isotropic equation of damage in incremental form. The Johnson-Cook model is incapable of predicting damage softening.

A value of  $D$  for a variety of materials can be computed inside the code EPIC II. Fracture is allowed when the damage parameter  $D$  reaches the value 1. For this material model,  $D$  is defined as,

$$D = \Sigma \frac{\Delta \epsilon^{vm}}{\epsilon^f} \quad (7)$$

Here  $\epsilon^{vm}$  represents the equivalent von Mises plastic strain. In Johnson-Cook (Johnson et. al., 1983), extensive dynamic tests were performed to estimate the model parameters. The data were obtained from torsion tests over a wide range of strain rates, from static tensile tests, from dynamic Hopkinson bar tensile tests and from Hopkinson bar tests at elevated temperatures.

#### *User Material Model*

In this work, we introduce the idea of damage softening in analogy with to thermal softening, making use of the effective stress concept applied to the constitutive equations of the material and to the yield stress criterion. The results presented in the last section are computed for adiabatic conditions, but illustrate the influence of the damage softening only.

Damage softening takes into account the fact that the deterioration of the material reduces its capacity to carry load. Mathematically, this concept is manifested by the inclusion of the damage parameter inside the constitutive equations of the material. This procedure assumes the existence of a damage-induced *equivalent stress*, which takes into account only the effective area that resists the load. Equation 8 better explains this idea. The basic notion is to introduce the damage parameter into the stress tensor, furnishing the equivalent effective stress.

$$\tilde{\sigma}_{ij} = \sigma_{ij}(1 - D) \quad (8)$$

The model introduced next is a variation of the Johnson-Cook model, which makes use of Equation 8 to incorporate of damage softening

$$\sigma = [A + B\epsilon^n] \left[ 1 + C \ln \epsilon^* \right] \left[ 1 - T^{*m} \right] (1 - D). \quad (9)$$

$$\epsilon^f = [D_1 + D_2 \exp D_3 \sigma] [1 + D_4 \ln \epsilon^*] [1 + D_5 T^*] \quad (10)$$

$$D = \Sigma \frac{\Delta \epsilon^{vm}}{\epsilon^f} \quad (11)$$

$$\epsilon^* = \frac{\dot{\epsilon}}{\dot{\epsilon}_0} \quad (12)$$

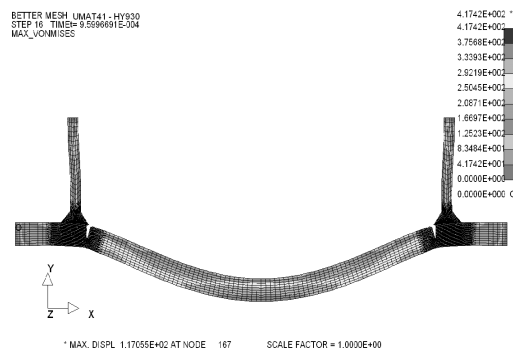


Fracture occurs when  $D$  reaches the value of 1.0. Equations 9 through 12 represent the problem to be numerically solved in the UMAT. Rigorously, new experimental tests should be performed in order to obtain new associated parameters  $A$ ,  $B$ ,  $C$ ,  $n$  and  $m$ . Here, however, for the sake of illustration, the same values are used as in Tables 1 and 2. Alternatively,  $D$  may be calculated using the formulations from Bonora (Bonora, 1997) or Lemaitre (Lemaitre, 1996).

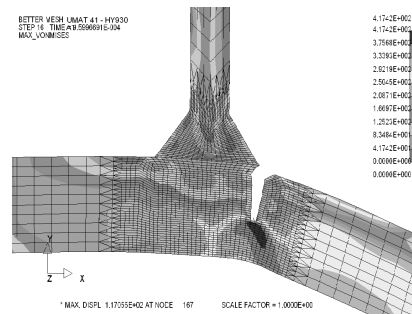
## RESULTS

The results presented in this work agree with previously published data (Giovanola, 1991, 1993), especially on the fracture path in a welded structure under dynamic load. As shown in the following pictures and tables, the expected softening behavior appears.

The next figures show some of the results from Table 3. Figure 7 shows the numerical results using the effective plastic strain model for the symmetric weld fillets under explosion loading equivalent to an initial velocity of 200m/s.



(a) Total fracture



(b) Detailed view of Figure (a)

Figure 7: Numerical Result – UMAT 41 – HY930 - under 200m/s

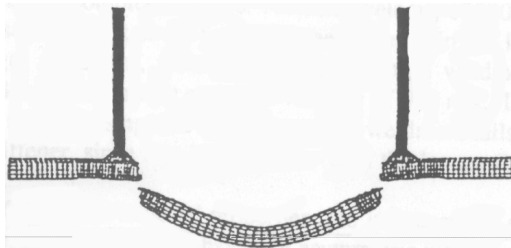
The results are qualitatively all consistent with previous published results; i.e., the appearance and path of the fracture are reproduced (see Table 3). For an initial velocity of 200m/s, however, when simulated with asymmetric weldment geometry, the material HY-930 shows different results for the MAT15 and UMAT41. At this point, this difference is attributed to damage softening effects. Experiments would be necessary to properly validate this particular numerical result. Although the models agree well on fracture path, the time histories obtained with and without damage softening are significantly different (Moraes et. al., 2000). We conclude that the strain rate effect is pronounced and cannot be neglected. This means that the models incorporating viscoplastic effects, rate effects in damage, and shear banding will agree with available qualitative data, such as fracture path, but are expected to give more realistic time history predictions.

Figure 8 shows numerical and experimental results, presented by Giovanola. In Table 3, they correspond to the symmetric weldment at 200m/s. The material properties come from Tables 1 and 2.

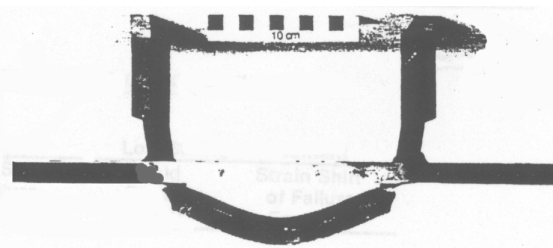
Figure 9 shows results obtained for 4340 Steel using the Johnson-Cook constitutive relations and material parameters extracted from the code EPIC II. Again, consistent results on fracture path are obtained when compared with other results available in prior literature.

Table 3: Initial Results

Weld Type	Material	Vo	Giovanola	MAT 15	UMAT 41
Symmetric	HY-930	100	No Fracture	No Fracture	No Fracture
		200	Fracture	Fracture	Fracture
Asymmetric	HY-930	100	No Fracture	No Fracture	No Fracture
		200 <sup>1</sup>	Fracture	Fracture	Fracture <sup>2</sup>
Symmetric	4340	100	Not Available	Fracture	Fracture
		200	Not Available	Fracture	Fracture



(a) Numerical Result



(b) Experimental result

Figure 8: Result obtained by Giovanola (Giovanola et. al., 1993).

Observe that Figures 7 and 9 are not comparable since they make use of different materials – Figure 9 uses 4340 Steel material and Figure 7 uses Giovanola’s material HY-930. However, the simulation of the materials under different models shows results qualitatively similar in terms of the location and the path of the fracture process.

Figure 10 represents the difference between the time history response for the different material models as previously discussed. Note: While the models agree qualitatively under respect to crack path, they differ substantially with respect to time history.

Similar results were also obtained for asymmetric weld geometries. Figure 11 shows the result for UMAT41. The particular geometry used in the numerical model shows results consistent with Giovanola, but it also shows fracture pattern differences as presented in Table 3. All simulations show fracture occurring in the HAZ. The fracture process can be total or partial.

<sup>1</sup> Different fracture processes were obtained.

<sup>2</sup> Partial fracture only

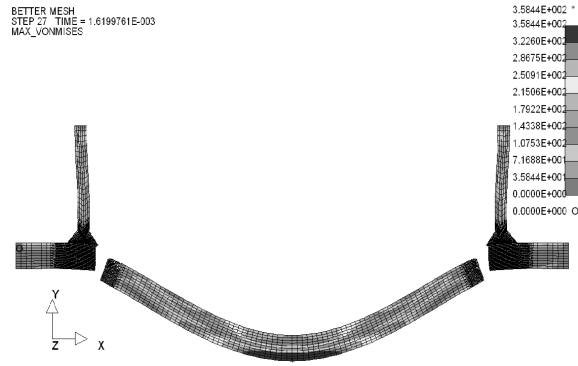


Figure 9: Symmetric weldment

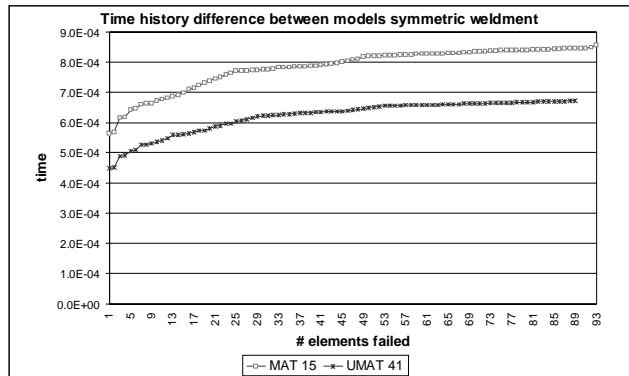


Figure 10: Time history comparison for  $V_0$  200m/s- Symmetric Weld (Note: Giovanola's result for this case: not available)

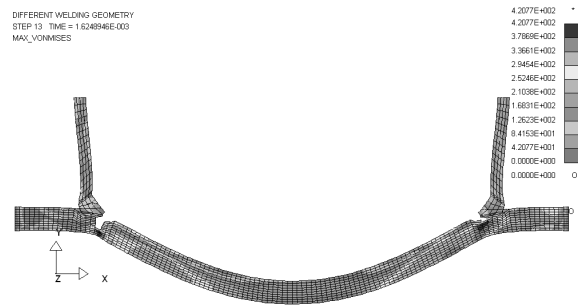
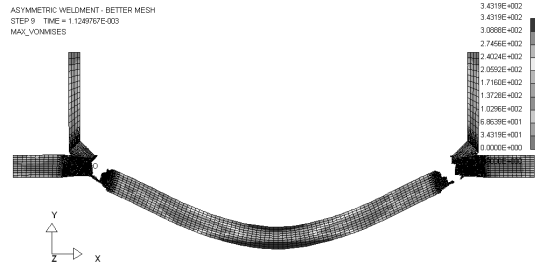


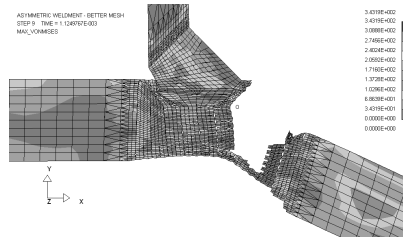
Figure 11: Asymmetric weldment - UMAT 41 – 200m/s

As stated before, this result is significantly different from the other results in Table 3. This outcome underpins the importance of performing numerical simulation on the constitutive equations of the materials. Recall that the models use different constitutive equations and that the failure criterion is not the same.

Figure 12 shows a similar simulation for 4340 Steel using the Johnson-Cook model. The results are once again consistent in terms of fracture path, but not quantitatively in terms of the time history. A similar graph showing the time history for the asymmetric weld geometry is presented in Figure 13.



(a) Johnson-Cook model



(b) Detailed view

Figure 12: Asymmetric weld – MAT 15 – 200m/s – 4340 Steel

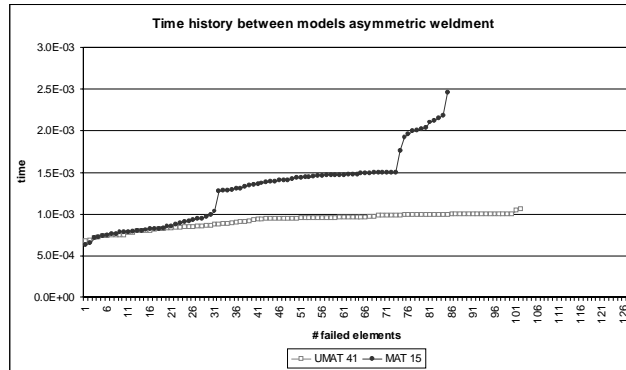


Figure 13: Time history comparison for  $V_0$  200m/s- Asymmetric Weld  
(Note: Giovanola's result for this case: not available)

### FINAL REMARKS AND CONCLUSION

A model able to accommodate damage and thermal softening in ductile fracture has just been introduced. We have shown that the use of the viscoplastic models and various damage models available in LS-DYNA leads to similar results in terms of occurrence of fracture and fracture pattern, for the majority of the examples shown here. However, in the cases where a deeper understanding of the dynamic process is required, for example thresholds, the time history must be analyzed.

The model is implemented in LS-DYNA finite element impact code as a UMAT. The UMAT is used to predict fracture of weldments under dynamic loading.

Experiments with recording techniques such as LCD cameras are required in order to properly validate the discussion on this work. Equipment with 100,000 – 500,000 frames/second should allow a good visualization of the dynamic fracture phenomena. Further development is also needed in the treatment of the variable  $D$ . Efforts are being concentrated in considering  $D$  as a 2<sup>nd</sup> order tensor  $D_{ij}$ . This would allow the analysis of non-metallic materials such as orthotropic composites.

## REFERENCES

BAMMAN, D. J., 'Modeling Temperature and Strain Rate Dependent Large Deformations of Metals', Appl. Mech. Rev., vol. 43, no 5, part2, May 1990.

BERSTAD, T., HOPPERSTAD, O. S., LADEMO, O-G and MALO, K. A., 'Computational Model of Ductile Damage and Fracture in Shell Analysis', 2<sup>nd</sup> European LS-DYNA Users Conference, Goetemburg, 1999.

BONORA, N., 'A Nonlinear CDM Model for Ductile Failure', Engineering Fracture Mechanics, vol. 58, no. ½, pp. 11-28, 1997.

GIOVANOLA, J.H., KIRKPATRICK, S.W., 'Methodology for Evaluating the Strength and Fracture Resistance of Weldments Using a Local Approach to Fracture', proceedings of the 1993 ASME PV&P, July 1993.

GIOVANOLA, J.H., KLOPP, R.W., Kirkpatrick, 'Dynamic Fracture of Welded Joints', proceedings of the DYMAT Conference, 1991.

HALLQUIST, J.O., Ls-Dyna Manuals, Livermore Software Tch. Co., 1993

JOHNSON, G. R. AND COOK, W. H., 'A Constitutive Model and Data for Metals Subjected to Large Strains, High Strain Rates and High Temperatures', 7<sup>th</sup> International Symposium on Ballistics, Netherlands, pp.541-547, April 1983.

KACHANOV, L. M., Introduction to Continuum Damage Mechanics, Martinus Nijhoff Publishers, 1986.

LEMAITRE, J., 'A Continuous Damage Mechanics Model for Ductile Fracture', Journal of Engineering Materials and Technology, vol. 107, pp. 83-89, 1985.

LEMAITRE, J., A Course on Damage Mechanics, 2nd ed., Springer, 1996.

MORAES, R. F., NICHOLSON, D. W., 'Simulation of the Time History of Fracture in Welded Joints under Impulsive Load', to be presented at the Southeastern Conference on Theoretical and Applied Mechanics (SECTAM XX), Auburn University, April 16-18, 2000.

MUDRY, F., 'Methodology and Applications of Local Criteria for the Prediction of Ductile Tearing', Elastic-Plastic Fracture Mechanics, pp. 263-283, 1985.

